


 CrossMark
click for updates

 Cite this: *Phys. Chem. Chem. Phys.*,
2016, **18**, 33226

Time-resolved photoelectron imaging of iodide–nitromethane ($I^- \cdot CH_3NO_2$) photodissociation dynamics†

 Alice Kunin,^a Wei-Li Li^a and Daniel M. Neumark^{*ab}

Femtosecond time-resolved photoelectron spectroscopy is used to probe the decay channels of iodide–nitromethane ($I^- \cdot CH_3NO_2$) binary clusters photoexcited at 3.56 eV, near the vertical detachment energy (VDE) of the cluster. The production of I^- is observed, and its photoelectron signal exhibits a mono-exponential rise time of 21 ± 1 ps. Previous work has shown that excitation near the VDE of the $I^- \cdot CH_3NO_2$ complex transfers an electron from iodide to form a dipole-bound state of $CH_3NO_2^-$ that rapidly converts to a valence bound (VB) anion. The long appearance time for the I^- fragment suggests that the VB anion decays by back transfer of the excess electron to iodide, reforming the $I^- \cdot CH_3NO_2$ anion and resulting in evaporation of iodide. Comparison of the measured lifetime to that predicted by RRKM theory suggests that the dissociation rate is limited by intramolecular vibrational energy redistribution in the re-formed anion between the high frequency CH_3NO_2 vibrational modes and the much lower frequency intermolecular $I^- \cdot CH_3NO_2$ stretch and bends, the predominant modes involved in cluster dissociation to form I^- . Evidence for a weak channel identified as $HI + CH_2NO_2^-$ is also observed.

 Received 28th September 2016,
Accepted 18th November 2016

DOI: 10.1039/c6cp06646a

www.rsc.org/pccp

1. Introduction

Anions with close-lying dipole bound (DB) and valence bound (VB) states are of considerable interest in understanding how closely spaced states with very different electronic properties are coupled to one another.^{1–3} This problem underlies the complex dynamics of low-energy electron attachment to nucleobases^{4–7} and, more generally, reductive damage to DNA.^{8–10} DB and VB transient anions formed by the capture of low energy electrons have been implicated in the cleavage of covalent bonds in DNA bases,^{6,11} but the roles of the two types of states are not yet fully understood. The coupling between DB and VB states and the apparent conversion of the DB anion to the VB anion of nucleobases has been observed experimentally^{1,12–14} and studied theoretically.^{15,16} Nitromethane, CH_3NO_2 , is also capable of forming both DB and VB negative ions,^{2,17} and as such it can serve as a model system to better understand the formation of and transition between DB and VB states in more complex molecules such as nucleobases. Negative ion photoelectron spectroscopy experiments on nitromethane are able to distinguish between the two anionic forms,¹⁷ and in our group, time-resolved photoelectron

imaging (TRPEI) experiments on binary clusters of iodide–nitromethane ($I^- \cdot CH_3NO_2$) have demonstrated complete and rapid conversion of the DB anion to the VB anion.¹⁸ In this work, we employ TRPEI with a higher energy probe pulse to investigate more closely the decay dynamics of $I^- \cdot CH_3NO_2$ clusters and examine the dissociation channels that lead to formation of I^- and other anion fragment products.

Nitromethane can capture low energy electrons to form DB anions through vibrational Feshbach resonances,^{19,20} and the VB anion is readily seen in the pulsed anion sources often used in photoelectron spectroscopy instruments.^{17,21} The C–NO₂ moiety is nearly planar in the DB anion, just as in neutral CH_3NO_2 ,²² but this group is pyramidal in the VB anion. The dissociative pathways of these anions have been investigated in dissociative electron attachment studies that have detected $CH_2NO_2^-$, NO_2^- , CH_3^- , and O^- fragments, among others.^{23,24} The nitromethane anion has also been shown to undergo rapid vibrational autodetachment following excitation of one quantum into any of the C–H stretching modes.²⁵ Weber and co-workers found that in clusters of nitromethane anions with methyl iodide, excitation of a C–H stretching mode in either constituent was able to induce dissociative electron transfer to form I^- fragments.²⁶

Binary clusters of iodide–nitromethane ($I^- \cdot CH_3NO_2$) have also been studied as a model system to examine the dynamics of electron capture and attachment to nitromethane and other species which are also capable of forming both DB and VB anions. Dessent and Johnson¹⁹ found that photoexcitation of

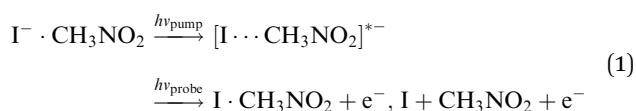
^a Department of Chemistry, University of California, Berkeley, CA, 94720, USA.
E-mail: dneumark@berkeley.edu

^b Chemical Sciences Division, Lawrence Berkeley National Laboratory, Berkeley, CA, 94720, USA

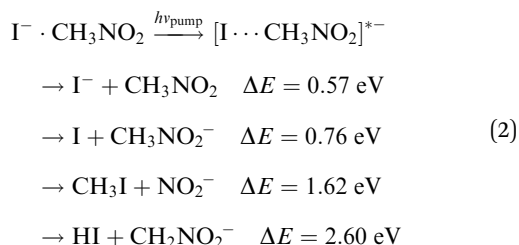
† Electronic supplementary information (ESI) available. See DOI: 10.1039/c6cp06646a

$\text{I}^- \cdot \text{CH}_3\text{NO}_2$ near its vertical detachment energy (VDE) of 3.60 eV yielded I^- and NO_2^- ion photofragments in a branching ratio of 25:1, a result that appeared to be approximately statistical when the clusters were analyzed in frequency groups using Rice–Ramsperger–Kassel–Marcus (RRKM) theory. In addition, a photofragment species that was suggested to be the CH_3NO_2^- DB anion was also observed, according to the results of field detachment studies.^{19,27} Our research group has carried out time-resolved experiments on $\text{I}^- \cdot \text{CH}_3\text{NO}_2$ clusters¹⁸ to gain insight into analogous experiments on iodide–nucleobase clusters, including iodide–uracil ($\text{I}^- \cdot \text{U}$),^{7,12,28} iodide–thymine,^{13,28} and iodide–adenine.¹⁴

In our previous TRPEI work on $\text{I}^- \cdot \text{CH}_3\text{NO}_2$ clusters, these species were excited with a femtosecond pump photon near the VDE of the cluster to initiate charge transfer from iodide to the nitromethane moiety and probed with a 1.56 eV near-infrared femtosecond probe pulse in the following scheme:



Formation of the cluster DB anion was observed within the cross-correlation of the pump and probe laser pulses.¹⁸ This DB feature was found to decay mono-exponentially on the order of 500 fs while the VB anion feature rise time was approximately 400 fs, providing experimental evidence that the DB anion acts as a “doorway” and decays to form the VB anion. The VB anion was found to decay bi-exponentially on the order of 2 ps and 1200 ps. This bi-exponential decay was attributed in part to autodetachment, which produces electrons with nearly zero kinetic energy. However, several other decay channels are also possible,^{18,19,27} including²⁹



In the present TRPEI study, a 3.14 eV probe pulse was used to interrogate $\text{I}^- \cdot \text{CH}_3\text{NO}_2$ clusters following photoexcitation near the cluster VDE. This higher probe photon energy makes it possible to observe the formation of dissociation products with larger electron binding energies (eBEs), including iodide (eBE = 3.059 eV) and NO_2^- (VDE = 2.273 ± 0.005 eV).³⁰ Photodetachment from I^- was observed with a rise time of 21 ± 1 ps. There is also evidence observed for weak production of the nitromethide anion, CH_2NO_2^- (VDE = 2.635 ± 0.010 eV).^{31,32} The DB and VB states of $\text{I}^- \cdot \text{CH}_3\text{NO}_2$ were also observed and measured to rise and decay with time constants similar to those of our previous work.¹⁸ The long iodide rise time was modeled using RRKM theory to calculate the statistical unimolecular decay lifetime of $\text{I}^- \cdot \text{CH}_3\text{NO}_2$ clusters, which were calculated to form

I^- in 294 fs following a pump excitation energy of 3.56 eV. The discrepancy between the experimental rise and the statistical result here may reflect weak coupling between intramolecular and intermolecular modes, leading to slowed intramolecular vibrational energy redistribution (IVR) in the cluster.^{33–36} The results here suggest that the VB anion decays not only *via* auto-detachment, but also by electron back-transfer to I to eventually evaporate I^- after slow IVR, and possibly *via* a minor alternative pathway to form HI and the nitromethide anion.

II. Experimental methods

The TRPEI apparatus has been described in detail previously,^{37,38} but is briefly summarized here. $\text{I}^- \cdot \text{CH}_3\text{NO}_2$ clusters were formed by passing 400 kPa of argon gas over a reservoir of iodomethane vapor and an ice-chilled reservoir of liquid nitromethane through a 500 Hz pulsed Even-Lavie valve equipped with a water-cooled jacket. The gas was supersonically expanded into vacuum through a ring electrode ionizer. The resulting anionic clusters were perpendicularly extracted using a Wiley-McLaren time-of-flight mass spectrometer³⁹ and mass-selected to isolate the desired $\text{I}^- \cdot \text{CH}_3\text{NO}_2$ binary clusters.

The mass-selected clusters were excited and photodetached by femtosecond ultraviolet pump and probe laser pulses whose delay was controlled by a delay stage. A KM Labs Griffin Oscillator and Dragon Amplifier generated 1 kHz, 40 fs pulses centered at 790 nm with 1.9 mJ per pulse. These were split between a Light Conversion TOPAS-C optical parametric amplifier to generate 11 μJ pump pulses at 3.56 eV (348 nm), and a frequency-doubling set-up to generate 30 μJ probe pulses at 3.14 eV (395 nm). The cross-correlation of the pump and probe laser pulses measured outside the chamber was approximately 185 fs.

Photoelectrons were analyzed using a velocity map imaging apparatus;⁴⁰ photoelectrons were detected using position-sensitive chevron-stacked microchannel plates coupled to a phosphor screen and imaged by a charge-coupled device camera. The photoelectron kinetic energy (eKE) distributions were reconstructed using the basis-set expansion (BASEX) method.⁴¹

III. Results

Photoelectron spectra of $\text{I}^- \cdot \text{CH}_3\text{NO}_2$ at 3.56 eV pump excitation energy and 3.14 eV probe energy are shown at selected delay times in Fig. 1. The spectra are dominated by two partially overlapped features, A and B, at eKE values below 0.2 eV, but there are several additional weak time-dependent features that are magnified in the various insets. Feature A, near zero eKE, is apparent at negative time delays when the probe precedes the pump pulse and also at zero delay, while feature B, at a slightly higher eKE of 0.08 ± 0.05 eV, grows in over tens of picoseconds and is very intense. The time-resolved photoelectron spectrum for the overlapped features A and B at 3.56 eV pump excitation energy and 3.14 eV probe energy is shown in Fig. 2; the y-axis is electron binding energy (eBE), where $\text{eBE} = h\nu_{\text{probe}} - \text{eKE}$.

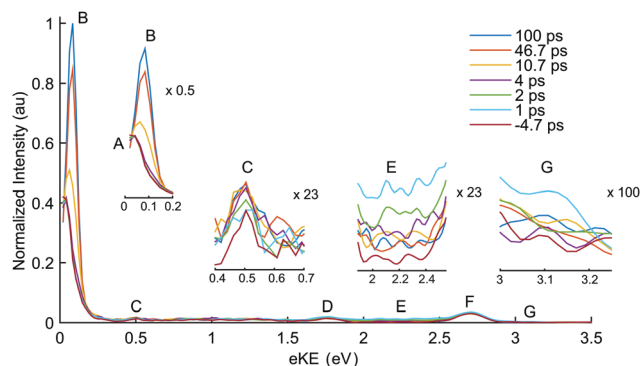


Fig. 1 Photoelectron spectrum of $\text{I}^- \cdot \text{CH}_3\text{NO}_2$ at 3.56 eV pump and 3.14 eV probe at selected delay times.

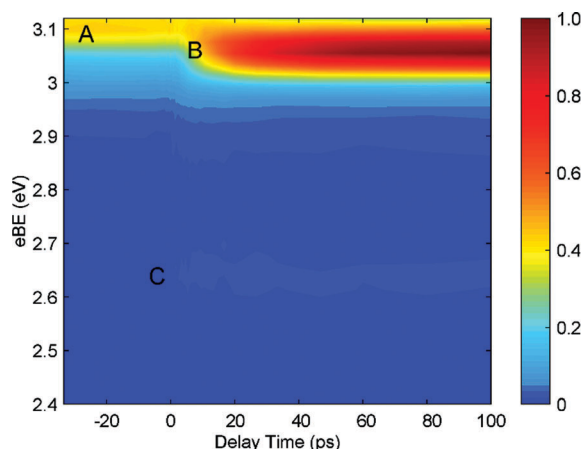


Fig. 2 Time-resolved photoelectron spectrum for features B (eBE = 3.06 eV) and C (eBE = 2.64 eV) at pump–probe delays for $\text{I}^- \cdot \text{CH}_3\text{NO}_2$ at 3.56 eV pump excitation energy and 3.14 eV probe energy.

This plot shows feature B growing in at an eBE of 3.06 eV. Fig. 3 shows the time-dependent normalized integrated intensity of feature B from the photoelectron spectrum in Fig. 2. Feature A is located near zero eKE and is present even in the absence of the probe pulse. Based on these attributes and our previous results, feature A is assigned to autodetachment from pump-excited $\text{I}^- \cdot \text{CH}_3\text{NO}_2$. From the binding energy of feature B, its narrow width,

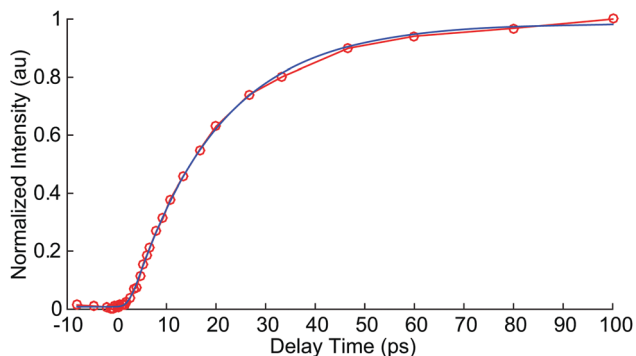


Fig. 3 Normalized integrated intensity of feature B from excitation at 3.56 eV vs. delay time. The rise time for feature B is 21 ± 1 ps.

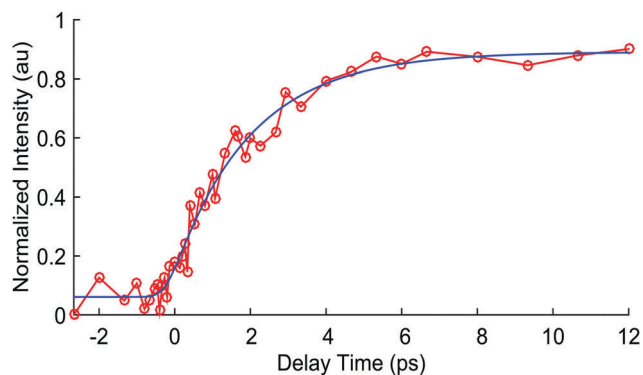


Fig. 4 Normalized integrated intensity of feature C at short time delays from excitation of 3.56 eV vs. delay time. The rise time for feature C is 2.1 ± 0.2 ps.

and its integrated time-dependence, we assign feature B to photo-detachment of atomic iodide produced by the dissociation of photoexcited $\text{I}^- \cdot \text{CH}_3\text{NO}_2$.

Feature C is a weaker time-dependent feature near 0.5 ± 0.05 eV eKE and appears to be relatively narrow as seen in the inset. Feature C is also apparent in Fig. 2 as a low intensity feature appearing at positive time delays with an eBE of 2.64 eV. The time-dependent normalized integrated intensity for the rise of feature C is shown in Fig. 4, and the long-time decay dynamics are shown in Fig. S1 (ESI[†]). Two of the larger remaining peaks in the spectrum, feature D near 1.75 eV and feature F near 2.7 eV, do not exhibit any time-dependence, so no inset is provided. The time-dependent and broad feature E, between 1.8 eV eKE and 2.6 eV eKE, has some contributions to its intensity on either side of this range from features D and F. Feature G, near 3.1 ± 0.1 eV eKE, is also time-dependent but very weak and narrow. The normalized integrated intensities showing the rise and decay dynamics for features E and G are shown in Fig. S2 and S3 (ESI[†]), respectively.

Feature C corresponds in eBE and in spectral shape relatively well to photodetachment from the bare nitromethide anion, CH_2NO_2^- ,³¹ which is an energetically accessible channel according to eqn (2). Features D and F correspond to direct detachment from $\text{I}^- \cdot \text{CH}_3\text{NO}_2$ by two probe photons to form $\text{I}(^2\text{P}_{1/2}) \cdot \text{CH}_3\text{NO}_2$ and $\text{I}(^2\text{P}_{3/2}) \cdot \text{CH}_3\text{NO}_2$, respectively. The eKEs of features E and G indicate that they are from probe-induced detachment from the VB and DB anions generated by the pump pulse, as discussed in our previously published results.¹⁸

IV. Analysis

To capture the rise and decay of features B, C, E, and G, the time-resolved signals are fit to the convolution of a Gaussian experimental response and multiple exponential functions using eqn (3).

$$I(t) = \frac{1}{\sigma_{\text{CC}}\sqrt{2\pi}} \exp\left(\frac{-t^2}{2\sigma_{\text{CC}}^2}\right) \cdot \begin{cases} I_0, & t < 0 \\ I_0 + \sum_i A_i \exp\left(\frac{-t}{\tau_i}\right), & t \geq 0 \end{cases} \quad (3)$$

I_0 is the signal background, σ_{CC} is the Gaussian full width at the half-maximum given by the cross-correlation of the pump and

probe laser pulses, A_i is the coefficient for each exponential term, and τ_i is the lifetime for each rise or decay exponential. Fig. 3 shows the fit of eqn (3) to the integrated intensity of Γ^- . The Γ^- feature has a mono-exponential rise time of 21 ± 1 ps and does not exhibit any decay. The fit to feature C, tentatively assigned to CH_2NO_2^- , is shown in Fig. 4 at delay times out to 12 ps, and longer time results are shown in Fig. S1 (ESI†). Feature C exhibits a rise time of 2.1 ± 0.2 ps, and fits to a mono-exponential decay which is longer than the timescale of this experiment (1000+ ps). Feature E, the VB anion, exhibits a rise time of 0.33 ± 0.15 ps and a bi-exponential decay of 2.2 ± 0.3 ps and 1100 ± 700 ps. Feature G, the DB anion, rises very quickly, within the cross-correlation of our pump and probe laser pulses, and decays mono-exponentially in 0.88 ± 0.22 ps. These rise and decay times for the DB and VB anions are within the error bars of our previously reported values, a cross-correlation limited DB rise and 0.63 ± 0.11 ps decay, and a VB rise of 0.37 ± 0.04 ps and bi-exponential decay of 2.3 ± 0.2 ps and 1100 ± 200 ps following photoexcitation at 3.55 eV.¹⁸ The results match relatively well despite the lower signal intensity for the DB and VB features in the present study.

The long lifetime of the Γ^- feature suggests a statistical mechanism may be relevant here, in which, for example, the iodide is ejected from highly vibrationally excited $\Gamma^- \cdot \text{CH}_3\text{NO}_2$ formed subsequent to UV excitation. To test this, we have employed Rice–Ramsperger–Kassel–Marcus (RRKM) calculations^{42,43} to model the lifetime for statistical unimolecular decay of $\Gamma^- \cdot \text{CH}_3\text{NO}_2$ to $\Gamma^- + \text{CH}_3\text{NO}_2$. RRKM theory calculates the microcanonical rate constant, $k(E)$, for statistical unimolecular dissociation for a species at a given energy E via eqn (4).

$$k(E) = \frac{G(E - E_0)}{h \cdot N(E)} \quad (4)$$

here $N(E)$ is the density of states of the reactant, $G(E - E_0)$ is the sum of states of the transition state, where E_0 is the zero point energy (ZPE) corrected energy difference between the reactant and transition state, and h is Planck's constant. E is the maximum energy provided to the system, taken to be the pump pulse energy.

The details of the calculations performed in this work using the Gaussian 09 computing package⁴⁴ may found in the ESI.† The calculated potential energy surface at the MP2/aug-cc-pVDZ level for dissociation of $\Gamma^- \cdot \text{CH}_3\text{NO}_2$ to form Γ^- and CH_3NO_2 is shown in Fig. S4 (ESI†). The calculated sum and density of states from the Beyer–Swinehart algorithm⁴⁵ and rate constant $k(E)$ for pump excitation at 3.56 eV are given in Table S1 (ESI†). The loose transition state expected for this reaction is located variationally, in order to yield the lowest calculated $k(E)$.⁴⁶ With corrections made to appropriately treat low-energy hindered internal rotor modes, RRKM theory calculates statistical unimolecular decay for $\Gamma^- \cdot \text{CH}_3\text{NO}_2$ to occur in approximately 294 fs following pump excitation at 3.56 eV, and with all modes simply treated harmonically this lifetime is 414 fs. This result is considerably faster than the experimental result of iodide rise time of 21 ± 1 ps following pump excitation at 3.56 eV; this discrepancy is explored in more detail in the following section.

V. Discussion

The work presented here provides new insights into the dynamics of photoexcited $\Gamma^- \cdot \text{CH}_3\text{NO}_2$ complexes. Using a higher probe photon energy, 3.14 eV, than in our previous TRPEI experiment, we are able to observe very prominent, time-dependent Γ^- production with a rise time of 21 ± 1 ps, as well as a much weaker feature that appears to correspond to CH_2NO_2^- production with a rise time of 2.1 ± 0.2 ps; neither of these species could be photodetached in our previous study at 1.56 eV probe energy. The cluster DB and VB anions are also observed, with similar time-dependence as reported previously.¹⁸

The intensity of the iodide signal in Fig. 1 is significantly greater than that of any other feature in the spectrum, even with the intensity of the autodetachment feature A removed. The iodide feature is approximately 30 times more intense than either the nitromethide anion or the VB anion, and 130 times more intense than the DB anion. The photodetachment cross section of iodide at 314 nm is approximately $3 \times 10^{-17} \text{ cm}^2$,⁴⁷ compared to a typical molecular cross section of approximately $0.7 \times 10^{-18} \text{ cm}^2$ for NO_2^- at 314 nm.⁴⁸ If the photodetachment cross section for the VB anion is similarly on the order of 10^{-18} cm^2 , this would indicate that despite its high photoelectron signal intensity, Γ^- is present in an approximately 1 : 1 ratio with the VB anion. Note that the VB CH_3NO_2^- anion may or may not be complexed with the neutral I atom; the two cannot be readily distinguished in our TRPE spectra.¹⁸ In any case, dissociation to $\Gamma^- + \text{CH}_3\text{NO}_2$ is a major channel whose dynamics are now accessible to our experiment.

We next examine possible mechanisms for Γ^- formation. Previous work applying TRPEI to iodide–uracil ($\Gamma^- \cdot \text{U}$) clusters showed that photoexcitation near the VDE transfers the excess electron to the uracil, forming a temporary negative ion that decays by autodetachment¹² and by back-electron transfer to the Γ^- ;⁴⁹ the latter process results in vibrationally excited $\Gamma^- \cdot \text{U}$ from which the Γ^- is ejected. A similar mechanism is likely for $\Gamma^- \cdot \text{CH}_3\text{NO}_2$, since photoexcitation is known to initiate electron transfer to the CH_3NO_2 , leading to a DB state that converts within approximately 500 fs to a VB state. The VB signal (also seen here as feature E) decays bi-exponentially with time constants of 2 ps and >1 ns. The amplitude of the VB signal drops by about 80% within 2 ps. Given the large Γ^- signal seen here, it seems reasonable to attribute most or all of this drop to back-electron transfer, re-forming $\Gamma^- \cdot \text{CH}_3\text{NO}_2$ which subsequently fragments.

The dissociation rate of $\Gamma^- \cdot \text{CH}_3\text{NO}_2$ to form Γ^- was found not to match the predictions of RRKM statistical unimolecular decay; the calculated and experimental lifetimes are 294 fs and 21 ps, respectively. In the case of $\Gamma^- \cdot \text{U}$, the RRKM lifetime of 8.6 ps was also less than the experimental lifetime of 86 ± 7 ps,⁴⁹ but the discrepancy here is about a factor of 7 larger. A key tenet of RRKM theory is that vibrational energy is randomly distributed and that this IVR is fast and complete on the timescale of the unimolecular reaction. This condition is unlikely to be satisfied given the sub-ps RRKM lifetime, suggesting that dissociation is not the rate-limiting step in Γ^- production even without considering

the discrepancy with experiment. Given the large disparity between the I^- experimental rise time and the RRKM statistical decay calculations presented here, either back-electron transfer or IVR must be the rate-limiting step to dissociation.

If back-electron transfer from the VB anion to reform $\text{I}^- \cdot \text{CH}_3\text{NO}_2$ is the rate-limiting step, there would need to be some charged, intermediate state corresponding to the precursor of $\text{I}^- \cdot \text{CH}_3\text{NO}_2$. While the dynamics of the $\text{I}^- \cdot \text{CH}_3\text{NO}_2$ electronic ground state species are challenging to observe uniquely from the direct detachment signal and the bare CH_3NO_2^- anion, there does not appear to be any signal in the TRPEI spectrum corresponding to a charged species from a delayed charge-transfer intermediate. Thus, we turn our attention to the process of IVR in the $\text{I}^- \cdot \text{CH}_3\text{NO}_2$ cluster.

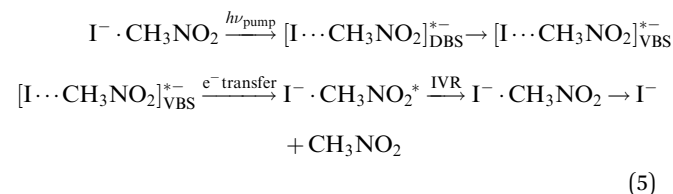
It is likely that back-electron transfer from the VB state of CH_3NO_2^- leads to considerable vibrational excitation of $-\text{NO}_2$ wagging and stretching modes in the re-formed $\text{I}^- \cdot \text{CH}_3\text{NO}_2$, since the C- NO_2 moiety is pyramidal in the VB anion and planar in the neutral. As determined by the calculations here† and presented in Table S2 (ESI†), $\text{I}^- \cdot \text{CH}_3\text{NO}_2$ clusters have three low frequency ($<100 \text{ cm}^{-1}$) modes corresponding to an iodide-nitromethane stretch and two approximately symmetric iodide-nitromethane bends. All other modes in the system are nitromethane internal vibrational modes with considerably higher frequencies, with the exception of the 27.4 cm^{-1} frequency associated with the internal methyl rotor. The question then is whether vibrational energy flow from the high frequency intramolecular modes excited by back-electron transfer into the low-frequency modes needed for dissociation will be the rate-limiting step for fragmentation to $\text{I}^- + \text{CH}_3\text{NO}_2$.

One can gain insight into this issue from the extensive experimental and theoretical studies of gas phase $\text{S}_{\text{N}}2$ reactions $\text{X}^- + \text{CH}_3\text{Y} \rightarrow \text{CH}_3\text{X} + \text{Y}^-$, where X and Y are typically halogen atoms but can also be molecular species.^{34,35,50} These reactions proceed *via* $\text{X}^- \cdot \text{CH}_3\text{Y}$ and $\text{Y}^- \cdot \text{CH}_3\text{X}$ ion-dipole complexes separated by a barrier. Classical trajectory calculations by Hase^{36,51} have shown that vibrational energy flow between the low-frequency intermolecular modes and high-frequency intramolecular modes of these complexes can be very inefficient and acts as a “dynamical bottleneck.” As a result, randomization of vibrational energy therefore often does not occur during the course of a reactive (or non-reactive) collision. This leads to non-statistical dynamics that are experimentally observable, such as deviations in the measured product angular and energy distributions from statistical models,^{52,53} or a non-statistical dependence of the rate constant on the internal energy of the reactants.⁵⁴

In the $\text{S}_{\text{N}}2$ studies, a bimolecular collision $\text{X}^- + \text{CH}_3\text{Y}$ collision is likely to lead to excitation of the low frequency intermolecular modes of the $\text{X}^- \cdot \text{CH}_3\text{Y}$ complex, with vibrational energy flow into the higher frequency intramolecular modes acting as a dynamical bottleneck. We propose that our experiment presents the opposite scenario, with the bottleneck between the initially excited CH_3NO_2 modes and the low-frequency $\text{I}^- \cdot \text{CH}_3\text{NO}_2$ intermolecular modes limiting the dissociation rate. This scenario has indeed been described in trajectory studies on the unimolecular dynamics of the $\text{Cl}^- \cdot \text{CH}_3\text{Br}$ and

$\text{Br}^- \cdot \text{CH}_3\text{Cl}$ complexes,³⁶ where, for example, the dissociation lifetime of the latter complex when there is significant intramolecular excitation was found to exceed 25 ps, considerably exceeding the calculated RRKM lifetime of 0.5 ps.

The following scheme describes the overall proposed mechanism:



Hase and co-workers are currently carrying out trajectory calculations on $\text{I}^- \cdot \text{CH}_3\text{NO}_2$ to test the proposed mechanism. We note that if the argument about the dynamical bottleneck limiting the dissociation of $\text{I}^- \cdot \text{CH}_3\text{NO}_2$ is confirmed, it is also likely to apply to the discrepancy between the experimental and RRKM dissociation lifetimes in $\text{I}^- \cdot \text{U}$.⁴⁹

In their investigation of the photoexcitation of $\text{I}^- \cdot \text{CH}_3\text{NO}_2$, Johnson and co-workers^{19,27} also observed formation of NO_2^- and CH_3NO_2^- anion photofragments. NO_2^- photofragments were reported to be observed in an approximately statistical 1:25 ratio with I^- photofragments. NO_2^- was not observed in the present TRPEI study, and given this branching ratio in addition to the cross sections cited above, photodetachment signal corresponding to NO_2^- is expected to be more than 1000 times weaker than the iodide signal observed here, essentially undetectable. The CH_3NO_2^- anion, if formed here, may not be distinguishable from the $\text{I}^- \cdot \text{CH}_3\text{NO}_2^-$ complex as the nitromethane VB anion and iodine-associated VB anion are similarly bound (eBE = 0.9 eV for CH_3NO_2^- VB anion),¹⁷ making it challenging to observe when photoelectron spectroscopy is the primary product characterization method.

A weak signal that appears to correspond to the nitromethide anion was also observed in the current experiment, indicating that a $\text{CH}_2\text{NO}_2^- + \text{HI}$ decay channel may also exist. In the $\text{I}^- \cdot \text{U}$ study, photofragment action spectra collected for $\text{I}^- \cdot \text{U}$ showed the formation of $[\text{U-H}]^-$ photofragments following photoexcitation near the VDE of the cluster, with I^- as the primary photofragment and $[\text{U-H}]^-$ as a minor product. $[\text{U-H}]^-$ was not observed in the time-resolved studies likely as a result of low production efficiency and a small photodetachment cross section for the species. In the present study, the possible formation of nitromethide anion in $2.1 \pm 0.2 \text{ ps}$ suggests that CH_2NO_2^- may form as part of the VB anion decay due to the close match-up of lifetimes. Note that the production of CH_2NO_2^- is only energetically accessible when the HI fragment is also formed; the C-H bond is too high in energy for CH_2NO_2^- to be a feasible product otherwise.

VI. Conclusions

TRPEI has been used to probe the decay dynamics of $\text{I}^- \cdot \text{CH}_3\text{NO}_2$ binary clusters excited at 3.56 eV, near the cluster VDE of 3.60 eV.

The formation of I^- was observed with a rise time of 21 ± 1 ps. This channel is attributed to photoexcitation in which the excess electron is transferred from the I atom to form $I-CH_3NO_2^-$, followed by back-electron transfer to re-form vibrationally excited $I^- \cdot CH_3NO_2$ that then dissociates to $I^- + CH_3NO_2$. Statistical calculations employing RRKM theory yield a substantially shorter lifetime of ~ 300 fs as compared to the experimental value, suggesting the presence of a dynamical bottleneck to unimolecular dissociation. This bottleneck is most likely from inefficient vibrational energy transfer from the intramolecular CH_3NO_2 vibrations excited by the back-electron transfer to the low-frequency intermolecular modes that must be energized for dissociation to occur. This result is commensurate with previous theoretical work on gas phase $X^- \cdot CH_3Y$ complexes for halogens. In addition, a weak signal associated with $CH_2NO_2^- + HI$ production was observed with a rise time of 2.1 ps.

Acknowledgements

This research was funded by the National Science Foundation under Grant no. CHE-1361412. A. K. gratefully acknowledges that this research was conducted with Government support under and awarded by DoD, Air Force Office of Scientific Research, National Defense Science and Engineering Graduate (NDSEG) Fellowship, 32 CFR 168a. The authors would like to thank W. L. Hase and X. Ma for helpful discussions regarding this work.

References

- J. H. Hendricks, S. A. Lyapustina, H. L. de Clercq and K. H. Bowen, *J. Chem. Phys.*, 1998, **108**, 8–11.
- R. N. Compton, H. S. Carman, C. Desfrancois, H. Abdoul-Carime, J. P. Schermann, J. H. Hendricks, S. A. Lyapustina and K. H. Bowen, *J. Chem. Phys.*, 1996, **105**, 3472–3478.
- T. Sommerfeld, *Phys. Chem. Chem. Phys.*, 2002, **4**, 2511–2516.
- S. Denifl, S. Ptasinska, G. Hanel, B. Gstir, M. Probst, P. Scheier and T. D. Mark, *J. Chem. Phys.*, 2004, **120**, 6557–6565.
- S. Denifl, S. Ptasinska, M. Probst, J. Hrušák, P. Scheier and T. D. Märk, *J. Phys. Chem. A*, 2004, **108**, 6562–6569.
- P. D. Burrow, G. A. Gallup, A. M. Scheer, S. Denifl, S. Ptasinska, T. D. Märk and P. Scheier, *J. Chem. Phys.*, 2006, **124**, 124310.
- M. A. Yandell, S. B. King and D. M. Neumark, *J. Am. Chem. Soc.*, 2013, **135**, 2128–2131.
- B. Boudaiffa, P. Cloutier, D. Hunting, M. A. Huels and L. Sanche, *Science*, 2000, **287**, 1658–1660.
- J. Simons, *Acc. Chem. Res.*, 2006, **39**, 772–779.
- J. D. Gu, J. Leszczynski and H. F. Schaefer, *Chem. Rev.*, 2012, **112**, 5603–5640.
- A. M. Scheer, C. Silvernail, J. A. Belot, K. Aflatooni, G. A. Gallup and P. D. Burrow, *Chem. Phys. Lett.*, 2005, **411**, 46–50.
- S. B. King, M. A. Yandell, A. B. Stephansen and D. M. Neumark, *J. Chem. Phys.*, 2014, **141**, 224310.
- S. B. King, A. B. Stephansen, Y. Yokoi, M. A. Yandell, A. Kunin, T. Takayanagi and D. M. Neumark, *J. Chem. Phys.*, 2015, **143**, 024312.
- A. B. Stephansen, S. B. King, Y. Yokoi, Y. Minoshima, W.-L. Li, A. Kunin, T. Takayanagi and D. M. Neumark, *J. Chem. Phys.*, 2015, **143**, 104308.
- T. Sommerfeld, *J. Phys. Chem. A*, 2004, **108**, 9150–9154.
- H. Motegi and T. Takayanagi, *THEOCHEM*, 2009, **907**, 85–92.
- C. L. Adams, H. Schneider, K. M. Ervin and J. M. Weber, *J. Chem. Phys.*, 2009, **130**, 074307.
- M. A. Yandell, S. B. King and D. M. Neumark, *J. Chem. Phys.*, 2014, **140**, 184317.
- C. E. H. Dessent, J. Kim and M. A. Johnson, *Faraday Discuss.*, 2000, **115**, 395–406.
- F. Lecomte, S. Carles, C. Desfrancois and M. A. Johnson, *J. Chem. Phys.*, 2000, **113**, 10973–10977.
- D. J. Goebbert, K. Pichugin and A. Sanov, *J. Chem. Phys.*, 2009, **131**, 164308.
- A. P. Cox and S. Waring, *J. Chem. Soc., Faraday Trans. 2*, 1972, **68**, 1060–1071.
- W. Sailer, A. Pelc, S. Matejcik, E. Illenberger, P. Scheier and T. D. Märk, *J. Chem. Phys.*, 2002, **117**, 7989–7994.
- E. Alizadeh, F. Ferreira da Silva, F. Zappa, A. Mauracher, M. Probst, S. Denifl, A. Bacher, T. D. Märk, P. Limão-Vieira and P. Scheier, *Int. J. Mass Spectrom.*, 2008, **271**, 15–21.
- C. L. Adams, H. Schneider and J. M. Weber, *J. Phys. Chem. A*, 2010, **114**, 4017–4030.
- B. J. Knurr, A. B. McCoy and J. M. Weber, *J. Chem. Phys.*, 2013, **138**, 224301.
- C. E. H. Dessent and M. A. Johnson, *J. Am. Chem. Soc.*, 1997, **119**, 5067–5068.
- S. B. King, M. A. Yandell and D. M. Neumark, *Faraday Discuss.*, 2013, **163**, 59–72.
- The ΔE values provided refer to the asymptotic energy difference between the indicated reactants and products, and were calculated in this work at the MP2/aug-cc-pVDZ level of theory using the Gaussian 09 computing package (ref. 44), as described in the following section and detailed in the ESI.†
- K. M. Ervin, J. Ho and W. C. Lineberger, *J. Phys. Chem.*, 1988, **92**, 5405–5412.
- R. B. Metz, D. R. Cyr and D. M. Neumark, *J. Phys. Chem.*, 1991, **95**, 2900–2907.
- The VDE is calculated from ref. 31 by $VDE = h\nu - eKE_{max}$ where $h\nu$ is the photon energy and eKE_{max} is the measured eKE of the maximum intensity peak of the photoelectron spectrum.
- P. Manikandan, J. Zhang and W. L. Hase, *J. Phys. Chem. A*, 2012, **116**, 3061–3080.
- W. L. Hase, *Science*, 1994, **266**, 998–1002.
- M. L. Chabinye, S. L. Craig, C. K. Regan and J. I. Brauman, *Science*, 1998, **279**, 1882.
- H. Wang, G. H. Peslherbe and W. L. Hase, *J. Am. Chem. Soc.*, 1994, **116**, 9644–9651.
- A. V. Davis, R. Wester, A. E. Bragg and D. M. Neumark, *J. Chem. Phys.*, 2003, **118**, 999–1002.
- A. E. Bragg, J. R. R. Verlet, A. Kammrath, O. Cheshnovsky and D. M. Neumark, *J. Am. Chem. Soc.*, 2005, **127**, 15283–15295.

- 39 W. C. Wiley and I. H. McLaren, *Rev. Sci. Instrum.*, 1955, **26**, 1150–1157.
- 40 A. Eppink and D. H. Parker, *Rev. Sci. Instrum.*, 1997, **68**, 3477–3484.
- 41 V. Dribinski, A. Ossadtchi, V. Mandelshtam and H. Reisler, *Rev. Sci. Instrum.*, 2002, **73**, 2634–2642.
- 42 T. Baer and W. L. Hase, *Unimolecular Reaction Dynamics: Theory and Dynamics*, Oxford University Press, New York, USA, 1996.
- 43 R. G. Gilbert and S. C. Smith, *Theory of Unimolecular and Recombination Reactions*, Blackwell Scientific Publications, London, 1990.
- 44 M. J. Frisch, G. W. Trucks, H. B. Schlegel, G. E. Scuseria, M. A. Robb, J. R. Cheeseman, G. Scalmani, V. Barone, B. Mennucci, G. A. Petersson, H. Nakatsuji, M. Caricato, X. Li, H. P. Hratchian, A. F. Izmaylov, J. Bloino, G. Zheng, J. L. Sonnenberg, M. Hada, M. Ehara, K. Toyota, R. Fukuda, J. Hasegawa, M. Ishida, T. Nakajima, Y. Honda, O. Kitao, H. Nakai, T. Vreven, J. A. Montgomery, Jr., J. E. Peralta, F. Ogliaro, M. Bearpark, J. J. Heyd, E. Brothers, K. N. Kudin, V. N. Staroverov, R. Kobayashi, J. Normand, K. Raghavachari, A. Rendell, J. C. Burant, S. S. Iyengar, J. Tomasi, M. Cossi, N. Rega, J. M. Millam, M. Klene, J. E. Knox, J. B. Cross, V. Bakken, C. Adamo, J. Jaramillo, R. Gomperts, R. E. Stratmann, O. Yazyev, A. J. Austin, R. Cammi, C. Pomelli, J. W. Ochterski, R. L. Martin, K. Morokuma, V. G. Zakrzewski, G. A. Voth, P. Salvador, J. J. Dannenberg, S. Dapprich, A. D. Daniels, Ö. Farkas, J. B. Foresman, J. V. Ortiz, J. Cioslowski and D. J. Fox, *Gaussian 09*, Gaussian Inc., Wallingford CT, 2009.
- 45 T. Beyer and D. F. Swinehart, *Commun. ACM*, 1973, **16**, 379.
- 46 J. I. Steinfeld, J. S. Francisco and W. L. Hase, *Chemical Kinetics and Dynamics*, Prentice-Hall, New Jersey, 1999.
- 47 R. S. Berry, *Chem. Rev.*, 1969, **69**, 533–542.
- 48 P. Warneck, *Chem. Phys. Lett.*, 1969, **3**, 532–533.
- 49 W.-L. Li, A. Kunin, E. Matthews, N. Yoshikawa, C. E. H. Dessent and D. M. Neumark, *J. Chem. Phys.*, 2016, **145**, 044319.
- 50 J. Xie, R. Otto, J. Mikosch, J. Zhang, R. Wester and W. L. Hase, *Acc. Chem. Res.*, 2014, **47**, 2960–2969.
- 51 G. H. Peslherbe, H. Wang and W. L. Hase, *J. Chem. Phys.*, 1995, **102**, 5626–5635.
- 52 S. T. Graul and M. T. Bowers, *J. Am. Chem. Soc.*, 1991, **113**, 9696–9697.
- 53 J. Mikosch, S. Trippel, C. Eichhorn, R. Otto, U. Lourderaj, J. X. Zhang, W. L. Hase, M. Weidemüller and R. Wester, *Science*, 2008, **319**, 183–186.
- 54 A. A. Viggiano, R. A. Morris, J. S. Paschkewitz and J. F. Paulson, *J. Am. Chem. Soc.*, 1992, **114**, 10477–10482.